IEEE Access
Multidisciplinary | Rapid Review | Open Access Journal

Received March 11, 2020, accepted March 26, 2020, date of publication March 31, 2020, date of current version April 16, 2020.

Digital Object Identifier 10.1109/ACCESS.2020.2984697

Implementation of Spatial/Polarization Diversity for Improved-Performance Circularly Polarized Multiple-Input-Multiple-Output Ultra-Wideband Antenna

UBAID ULLAH[1], ISMAIL BEN MABROUK[1], (Senior Member, IEEE), SLAWOMIR KOZIEL[2,3], (Senior Member, IEEE), AND MUATH AL-HASAN[1], (Senior Member, IEEE)

[1]Networks and Communication Engineering Department, Al Ain University, Abu Dhabi, United Arab Emirates
[2]Engineering Optimization and Modeling Center, Reykjavik University, 101 Reykjavik, Iceland
[3]Faculty of Electronics, Telecommunications and Informatics, Gdansk University of Technology, 80-233 Gdansk, Poland

Corresponding author: Ubaid Ullah (ubaid.ullah@aau.ac.ae)

This work was supported in part by the Abu-Dhabi Department of Education and Knowledge (ADEK) Award for Research Excellence 2019 under Grant AARE19-245, in part by the Icelandic Centre for Research (RANNIS) under Grant 206606051, and in part by the National Science Centre of Poland under Grant 2018/31/B/ST7/02369.

ABSTRACT In this paper, spatial and polarization diversities are simultaneously implemented in an ultra-wideband (UWB) multiple-input-multiple-output (MIMO) antenna to reduce the correlation between the parallel-placed radiators. The keystone of the antenna is systematically modified coplanar ground planes that enable excitation of circular polarization (CP). To realize one sense of circular polarization as well as ultra-wideband operation, an extended rectangular slot is etched on the left-hand-side of the coplanar waveguide (CPW) feed. This is combined with the asymmetrical ground plane geometry on the right-hand-side of the feeding line. The current flowing on the slotted ground plane forms a quasi-loop and generates CP, whereas the combination of the vertical current on the feedline and the horizontal current on the asymmetric ground plane adds to the axial ratio (AR) bandwidth. To implement the MIMO design with polarization and spatial diversity, the position of the coplanar ground planes is switched with respect to the feedline, and placed in a parallel formation with the edge-to-edge distance of $0.29\lambda_0$. All geometrical parameters are optimized at the full-wave level of description before prototyping and experimental characterization. Simulation and measured results indicate that the proposed MIMO antenna features approximately 82% impedance bandwidth from 2.9 GHz to 7.1 GHz and 68.5% (3.1 GHz- 6.35 GHz) AR bandwidth. Moreover, the peak envelop correlation coefficient (ECC) is below 0.003, which corresponds to almost no correlation between the radiators. The antenna can be operated with either bidirectional or unidirectional characteristics, covering multiple commercial application bands including WLAN and WiMax.

INDEX TERMS Circular polarization antennas, MIMO antennas, compact antennas, wideband antennas, simulation-driven design.

I. INTRODUCTION

Owing to the multiple-input-multiple-output (MIMO) technology, the modern wireless communication era has witnessed enormous improvement in the spectral efficiency and robustness of the wireless communication links [1], [2]. The MIMO systems transmit and receive multiple streams of data over multiple channels, which improves the link reliability, data rates and the channel capacity while employing limited power and bandwidth. Moreover, the MIMO systems have demonstrated a capacity to dramatically increase the overall system capacity, particularly in a rich multipath environment [3]–[5]. The long time maturity of MIMO wireless communications technology can be inferred from the state of current wireless communication systems. It has shown signs of becoming a major factor in the increased productivity

The associate editor coordinating the review of this manuscript and approving it for publication was Bilal Khawaja.

demands from industry and it is a major enabling factor in the growing prominence of the signal reliability and the overall system capacity in the current 4G wireless standard as well as the forthcoming 5G and 6G standards. Furthermore, this technology is expected to be the key enabler for long-envisaged, compact, highly integrated autonomous applications in various sectors [6].

The design of modern and improved MIMO antenna systems has been fostered by the aforementioned advancements in wireless industry. In particular, the performance of the MIMO system can be further improved by establishing parallel sub-channels provided that the data transmitted and received is uncorrelated [7], [8]. The antenna correlation can be diminished by implementing various decoupling and isolation techniques for reducing mutual coupling between the radiators. The shortcomings of these techniques include added complexity and the cost of the circuit [9]–[11]. An alternative solution to reduce correlation and to improve the system capacity is a utilization of diversity techniques. In the multi-path channels, the signal fading is caused by the interference from the reflected signal which severely affect the reliability of the received signal. The signal fading can be decreased by using divers systems by using diversity combining [12]. Spatial diversity is an effective approach to improving antenna isolation and hence reducing the correlation between the MIMO antennas. In this technique, the antennas are physically separated from each other with the minimum acceptable edge-to-edge distance of half of a wavelength [11], [13]. The drawback of this technique, particularly pertinent to electrically large antennas, is the undesired increase of the physical size of the structure. In [14]–[16], it has been established that by implementing various diversities, including pattern and polarization ones, or the combination thereof, can improve the performance of the MIMO system by reducing the correlation between the transmitted/received data signals. However, majority of the antenna designs in the literature are either linearly polarized (LP) or operate in a very narrow band hence limiting the capacity of wireless communication systems, especially in a dense multipath environment.

On the other hand, circularly polarized (CP) antennas are known for their strong immunity to multipath effects, absorption losses, signal attenuation, mismatch losses and low sensitivity to physical orientation [17]–[22]. The effect of circular polarization diversity on the capacity of a MIMO system has been studied in [23] using a polarization reconfigurable antenna. It has been demonstrated that in contrast to LP antenna diversity, CP antenna with polarization diversity can significantly increase the system performance particularly in the line of sight (LOS) scenario. Although polarization reconfigurable antennas can be deemed suitable for MIMO applications, switching between the polarization states requires additional active circuit components, making the antenna circuit cumbersome and costly.

In this paper, polarization and spatial diversities are combined to design an ultra-wideband circularly polarized MIMO antenna with almost no correlation between the radiators. The proposed design is based on a carefully shaped coplanar waveguide fed slot structure. One side of asymmetrically printed coplanar ground plan is etched to form a slot and to generate a guided quasi-loop path for the current flow. This induces one sense of circular polarization in the antenna. To further broaden the axial ratio (AR) bandwidth, the horizontal current on the shortened ground plane and the vertical current on the quarter wavelength microstrip line monopole are combined to form a tilted current and to generate an additional CP mode. The advantage of this design is the ease of changing the sense of polarization from right-hand CP (RHCP) to the left-hand CP (LHCP), by simply switching the position of the ground plane with respect to the feed line. For realizing the MIMO antenna with circular polarization diversity, the two antennas are placed parallel with edge-to-edge distance of only $0.29\lambda_0$. The total footprint of the single antenna is only $0.34\ \lambda_0 \times 0.38\ \lambda_0 = 0.13\lambda_0^2$ with the total size of the MIMO structure of $0.34\lambda_0^2$ when calculated at the lowest operating frequency. The electrically small size of the individual antenna element reduces the edge-to-edge spatial distance from the conventional half wavelength to less than one third of the wavelength. A low level of envelop correlation coefficient (ECC) evaluated from the far field is below 0.003 can be attributed to the combination of spatial and polarization diversity. Overall, the antenna features a wide impedance and axial ratio bandwidth with stable bidirectional/unidirectional radiation characteristics.

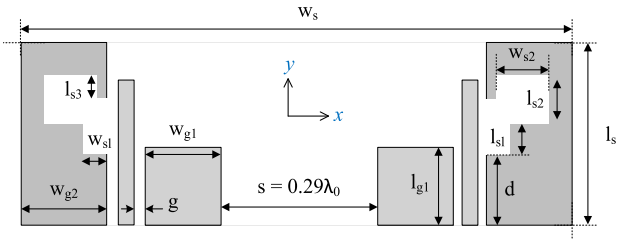

FIGURE 1. Geometry of the proposed CP MIMO antenna.

II. ANTENNA DESIGN AND ANALYSIS

A. ANTENNA DESIGN AND MIMO IMPLEMENTATION

The geometry and parameterization of the proposed antenna has been shown in Fig. 1. The antenna is printed on single-sided laminated Rogers RO4003 substrate (permittivity $\varepsilon_r = 3.38$, tangent loss $\tan\delta = 0.0027$, thickness $h = 0.813$ mm). In the first step, a single-element ultra-wideband CP antenna is designed by systematic modifications of the conventional coplanar waveguide coplanar ground planes. A 50-ohm quarter-wavelength microstrip line monopole with the length $l_m = 26$ mm and a coplanar gap $g = 0.6325$ mm is used to excite the antenna. The microstrip line monopole is designed to operate with the lower cut-off frequency of 3 GHz. The symmetry of the coplanar ground planes is broken along the longitudinal direction of the excitation line and a slot is etched in the elongated ground plane to form a quasi-loop. For exciting RHCP, the slotted ground

TABLE 1. Final (optimized) parameter values in mm.

Parameter	Value	Parameter	Value	Parameter	Value
l_s	33.5	l_{sl}	7.31	l_{s2}	10.49
w_s	99.73	w_{sl}	3.90	w_{s2}	7.48
l_{g1}	14.52	l_{g2}	33.5	L_m	26.0
w_{g1}	15.81	w_{g2}	17.18	l_{s3}	4.73
g	0.6325	d	10.76	w_{s3}	1.74

plane is located on the left-side of the feedline, whereas for inducing LHCP in the same antenna, the position of the ground planes is mirrored with respect to the feedline as depicted in the Fig. 1. The external dimensions of the two-element MIMO antenna are $w_s \times l_s = 99.7$ mm $\times$ 33.5 mm. For isolation $|S_{21}| \geq -20$ dB, the two antennas are placed in parallel with edge-to-edge distance of 28.9 mm which corresponds to approximately one-third of the wavelength at the lowest operating frequency of the antenna. The computational model of the antenna is implemented and simulated using CST Microwave Studio and optimized at the full-wave level of description. The final values of the geometry parameters are listed in Table 1. The proposed MIMO antenna can be operated with bidirectional radiation characteristics with polarization diversity in each direction. Additionally, the antenna is made to operate with polarization diversity in a directional manner by placing a flat metallic reflector behind the antenna. For constructive interference of the reflected signal, the minimum distance of the reflector is a quarter wavelength.

B. CIRCULAR POLARIZATION MECHANISM

For inducing CP diversity and to retain simplicity of the circuit, the proposed two-element MIMO antenna is implemented in a parallel formation. To explain the circular polarization mechanism and the polarization diversity, the magnetic surface current distribution is shown in Fig. 2(a).

When Port 1 (left-hand-side) is excited, the antenna operates with right-hand circular polarization. The quasi-loop formed in the left-side ground plane by the etched slot creates a path for the current flow generating one sense of CP. The current flow highlighted using arrows indicates formation of the loop-like structure in the counter-clockwise direction as illustrated in Fig. 2(a). It is well-known that traveling wave current distribution forming a loop generates circular polarization [24]. The axial ratio (AR) bandwidth is further extended by the additional CP mode shown in Fig. 2(b). The position of the dominant field components is shown for different angular times at 5 GHz. The vertical current components on the microstrip line monopole and the horizontal current on the ground plane form orthogonal currents with the phase progression, and generate additional CP. For reproducing the same antenna with left-hand circular polarization, the position of the coplanar ground planes is simply switched with respect to the microstrip line. The direction of the current highlighted using arrows illustrates the clockwise rotation of the current; consequently, left-hand CP is realized. The same phenomenon occurs for the additional CP mode

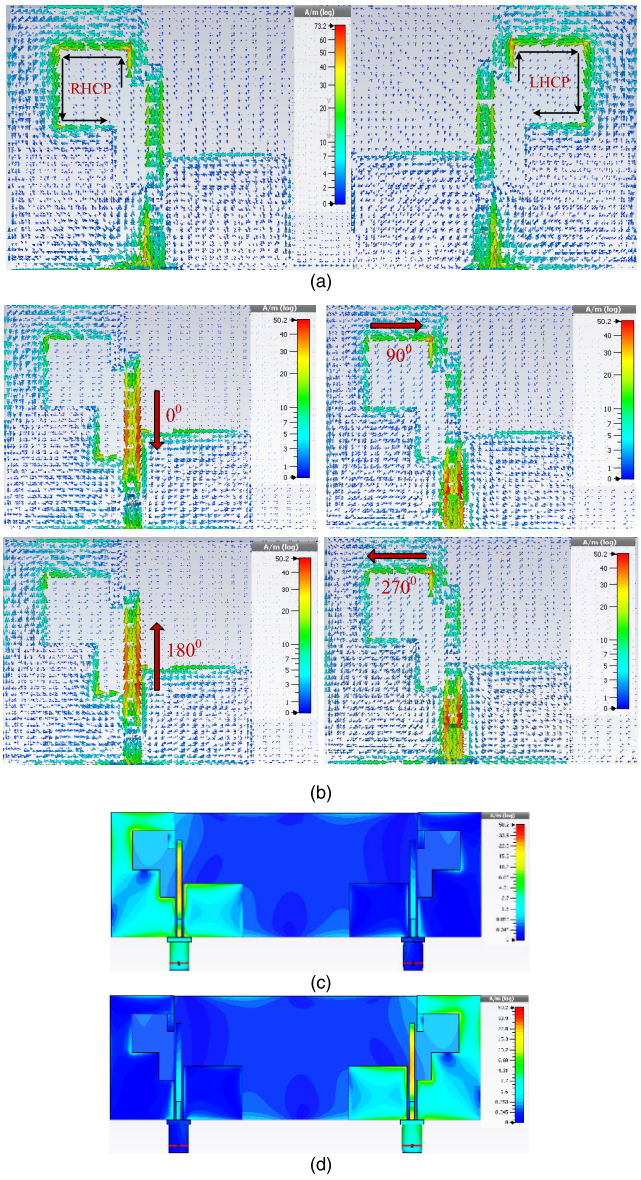

FIGURE 2. (a) Circular polarization mechanism of the proposed antenna with magnetic current distribution at 3.5 GHz; (b) magnetic current at 5 GHz (c) Port 1 surface current; (d) Port 2 surface current.

generated by the asymmetrical ground plane and the feedline. To illustrate the port-to-port isolation, the absolute surface current distribution is shown in Figs. 2(c) and 2(d). It can be seen that the amount of energy leaking from one port to another is very small. The average achieved isolation level is below –20 dB (with the edge-to-edge distance of one third of the wavelength), which is attributed to the small size of the antenna elements.

C. BIDIRECTIONAL RADIATION PATTERN

The proposed antenna can be operated with both unidirectional and bidirectional radiation characteristics. To illustrate the bidirectional behavior of the antenna, the radiation patterns for both ports is shown in Fig. 3 at 3.5 GHz and 5.5 GHz. The antenna excited from Port 1 radiates RHCP in the +z-direction and LHCP in the –z-direction

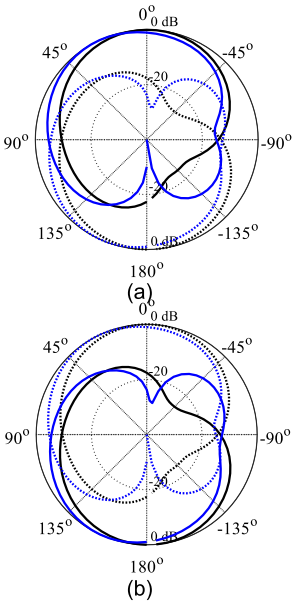

FIGURE 3. Radiation pattern of the proposed antenna. RHCP (solid) and LHCP (dashed): (a) Port 1 3.5 GHz (black) and 5.5 GHz (blue) and (b) Port 2 3.5 GHz (black) and 5.5 GHz (blue).

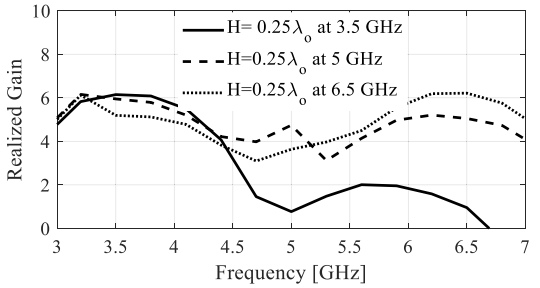

FIGURE 4. Realized gain versus reflector distance.

while the antenna excited from Port 2 radiates LHCP in the +z-direction and RHCP in the –z-direction. It is can be observed that the pattern in each direction is the same with a slight tilt away from the broadside direction. The minor beam tilt is due to the asymmetrical and hence uneven current distribution on the ground planes.

The average realized gain of the antenna when operated without a reflector is 3.04 dBic. With the directional radiation pattern, the proposed antenna can be used for several indoor applications including tunnels, underground mines and subways.

D. ANTENNA REALIZED GAIN VS. REFLECTOR DISTANCE

This section investigates the dependence of antenna gain on the reflector distance. The primary condition for the reflector to work effectively is to maintain its distance from the antenna equal to the quarter wavelength. The size of the reflector also plays a vital role in reflecting the electromagnetic energy into a particular direction. Due to the wideband nature of the antenna and the finite size of the reflector, the aforementioned condition can only be met for a certain frequency band. The analysis in Fig. 4 indicates that the realized gain does vary

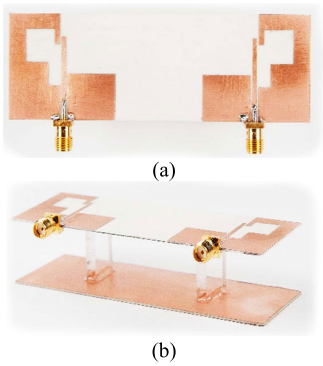

FIGURE 5. Antenna prototype and the characterization setup: (a) Front view, (b) Perspective view.

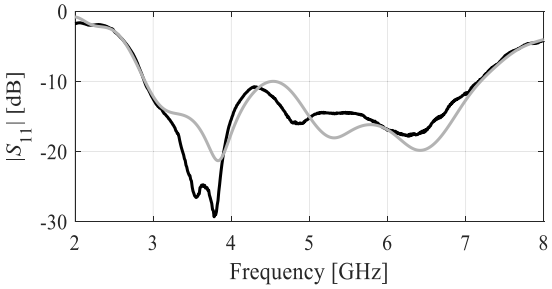

FIGURE 6. Reflection response $|S_{11}|$: simulation (gray) and measurement (black).

with the reflector distance. It is important to mention here that near 5 GHz, the radiated fields are dominated by the microstrip line monopole (cf.2(b)) which is of low gain due to omnidirectional radiation characteristics. The antenna is optimized and characterized only for 3.5 GHz distance. Note that the antenna AR bandwidth is adversely effected when only the reflector distance is adjusted.

This shows that all the antenna adjustable parameters need to be re-optimized if other values of reflector distance are to be used.

III. NUMERICAL RESULTS AND EXPERIMENTAL VALIDATION

A. S-PARAMETERS AND AXIAL RATIO

The prototype of the proposed MIMO antenna with circular polarization diversity is shown in Fig. 5. The antenna has been characterized in the anechoic chamber of Reykjavik University, Iceland, for all major performance figures. Due to identical structure of both radiators, the characterization of the antenna is only performed for one port with the second port terminated with a 50-ohm load. The simulated and measured reflection coefficient $|S_{11}|$ is shown in Fig. 6. The results indicate that the antenna features wide a impedance bandwidth of up to 82% from 2.9 GHz to 7.1 GHz. Another very important performance metric is the isolation between the two antennas.

The simulated and measured $|S_{21}|$ of the antenna is illustrated in Fig. 7. The averaged isolation value achieved is well

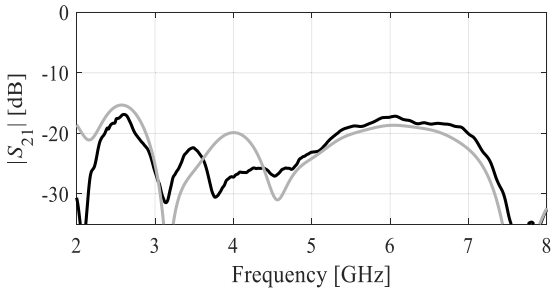

FIGURE 7. Isolation characteristic $|S_{21}|$: simulation (gray) and measurement (black).

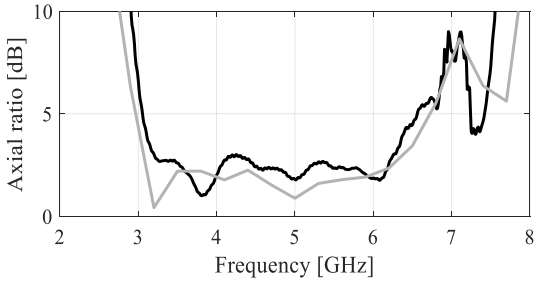

FIGURE 8. Axial ratio AR: simulation (gray) and measurement (black).

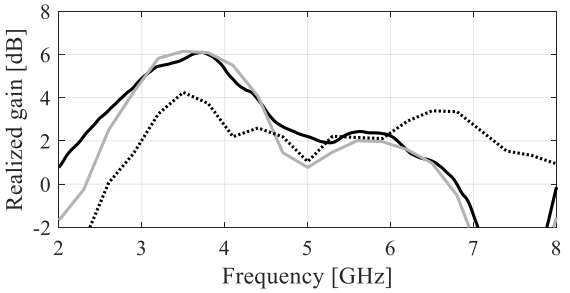

FIGURE 9. Realized gain with reflector: simulation (gray) and measurements (black), without reflector (….).

below –20 dB. This is realized with the edge-to-edge distance of only 0.29 λ_0. It is important to emphasize here that the total footprint of the individual antenna is only a fraction of the wavelength when calculated at the lower cut-off frequency. The improved isolation level is attributed to the relatively small size of each antenna element and the intrinsically uncorrelated nature of the polarization diversity. The axial ratio of the antenna is illustrated in Fig. 8. The measured results demonstrate that the proposed MIMO antenna features a wide axial ratio bandwidth of approximately 68.5% covering the frequency range from 3.1 GHz to 6.35 GHz.

B. REALIZED GAIN AND EFFICIENCY

The simulated and measured realized gain of the antenna with reflector is shown in Fig. 9. As the function of the reflector is to reflect the electromagnetic energy and redirect it to the broadside direction, the distance of the reflector from the antenna should be a quarter wavelength. The peak realized gain achieved for the proposed antenna is approximately 6 dBic when the distance is set according to the

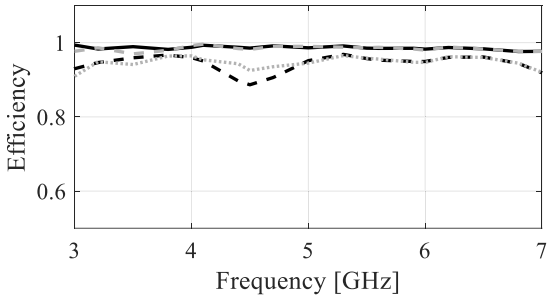

FIGURE 10. Simulation (gray) and measured (Black) antenna radiation efficiency (—) and total efficiency (- - -).

lower cut-off frequency. The average realized gain without the reflector is 3.04 dBic. Due to the wideband nature of the antenna, the reflector distance conditioned to a quarter wavelength can only cover part of the spectrum. The gain can be further improved by implementing a large size cavity on integrating the antenna a sidewall of a large object such as a vehicle or train. The radiation and the total efficiency of the antenna is depicted in Fig. 10. The average in-band radiation efficiency of the antenna is 98% with peak value reaching up to 99.7%. Moreover, the total average efficiency of the antenna is approximately 92%.

C. RADIATION PATTERN ANALYSIS

The radiation pattern of the antenna is characterized with the integrated flat reflector behind the radiator, which guides all the electromagnetic energy to the broadside direction. The radiation characteristics are analyzed in the two principal planes, the xz- and yz-plane, at three frequency frequencies, i.e. 3.5 GHz, 4.5 GHz and 5.5 GHz for Port 1 with Port 2 is terminated by a matching load.

The orientation of the antenna is according to the coordinate system given in Fig. 1. The sense of polarization of Port 1 is RHCP in the $+z$-direction and LHCP in $-z$-direction. The normalized results in the form of polar plots are depicted in Fig. 11 which shows stable radiation characteristics of the co-polarized fields in the $+z$-direction. A minor beam tilt away from the broadside is attributed to the asymmetrical topology of the coplanar ground plane. The cross-pol level is well below the co-pol particularly in the broadside direction. This shows the suitability of the proposed MIMO antenna for applications requiring directional antennas. The radiation pattern of port is similar to port one, with the only difference being the sense of polarization.

D. ENVELOPE CORRELATION COEFFICIENT AND DIVERSITY GAIN

In the MIMO wireless communication systems, ECC is one of the major figures of merit used for quantifying the performance in terms of diversity. This parameter can be evaluated from the scattering parameters of the ports, but this is only applicable to highly efficient antennas. Due to the wideband

TABLE 2. Comparison with State-of-The-Art MIMO antennas.

Reference	Operating frequency (GHz)	Diversity type	Polarization	Size [λ_o^2]	Isolation (dB)	Peak Gain (dBic)	%AR	%BW
[3]	5.5	Polarization	Circular	0.25	13	~4.5	4.7	----
[11]	3.3	Polarization	Linear	0.61	25	4	----	28.5
[12]	5.3	Polarization	Linear/Circular	0.43	18	2.85	2.32	16.28
[26]	2.4	Polarization	Dual	0.09	12	2.79	----	20
[27]	5.2	Polarization	Circular	0.16	22	5.8	18.3	18.3
[28]	2.4/5.15	---	Linear	0.26	15	----	----	8.2
Proposed	3	Polarization	Circular	0.34	22	6	68.5	82

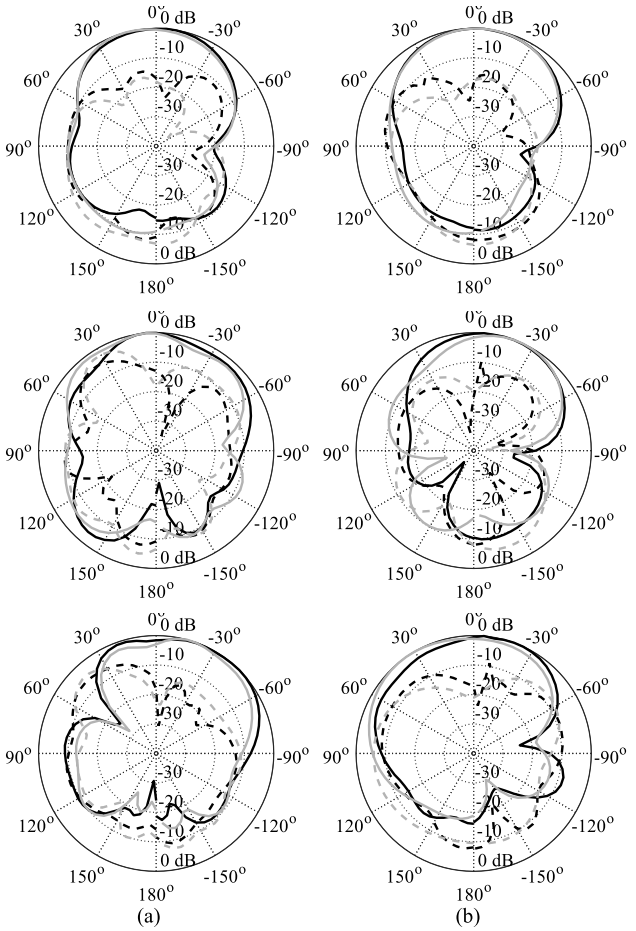

FIGURE 11. Simulation (gray) and measured (black) normalized radiation pattern of the proposed MIMO antenna at 3.5 GHz, 4.5 GHz and 5.5 GHz respectively (a) *xz*-plane (b) yz-plane.

nature of the antenna at hand, the efficiency varies across the operating band.

Additionally, the channel capacity of the communication system is not affected directly by the port scattering parameters, rather by the spatial behavior of the antenna. Therefore, the ECC is evaluated from the far-field pattern over a sphere using the following formula.

$$\rho e = \frac{|_{4\pi}\left[\vec{F}_i(\theta,\phi) * \vec{F}_j(\theta,\phi)\right] d\Omega|^2}{_{4\pi}|\vec{F}_i(\theta,\phi)|^2 *_{4\pi} \vec{F}_j(\theta,\phi)|^2} \quad (1)$$

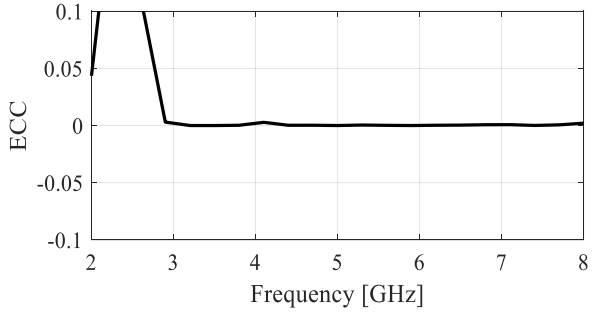

FIGURE 12. Calculated Envelop Correlation Coefficient.

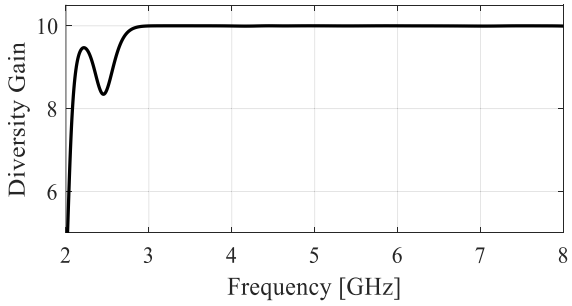

FIGURE 13. Calculated diversity gain.

The calculated ECC results shown in Fig. 12 indicate that there is almost no correlation between the two relatively closely space antennas. The diversity gain (DG) is another performance figure that measures the enhancement in the signal to noise ratio (SNR). The signal received through different branches of the communication network is collected and the SNR is calculated. Through DG analysis, the improvement offered by the MIMO antenna compared to single-input-single-output (SISO) can be estimated. It is important to mention here that there is a direct relation between the ECC and DG, which is

$$DG = 10\sqrt{1 - |0.99\rho e|^2} \quad (2)$$

The DG is calculated using (2) and the corresponding results are shown in Fig. 13. It can be observed that the proposed antenna offers almost 99.9 DG.

E. BENCHMARKING

For comprehensive benchmarking, the proposed MIMO antenna is compared with the recent state-of-the-art designs.

The comparison is done based on several major performance figures including the type of diversity adopted, polarization of the antenna, the overall radiator size (calculated with respect to the lower cut-off frequency), the level of isolation, peak realized gain, AR bandwidth and the impedance bandwidth. The data related to referenced designs is gathered in Table 2. For impartial comparison, the lowest operating frequencies are also included in the table. It can be observed that the proposed MIMO antenna outperforms the referenced designs in almost all fronts except the size, which is fractionally large. But due to the fact that other figure of merits, particularly the AR bandwidth and the impedance bandwidth of the proposed antenna are significantly wider, the slightly larger size can be considered as a trade-off between the footprint and the overall (both electrical and field) performance.

IV. CONCLUSION

In this paper, an ultra-wideband circularly polarized MIMO antenna with polarization and spatial diversity is presented. The polarization diversity is implemented by first designing a CP antenna with one sense of polarization. A coplanar waveguide feeding is used with asymmetrical ground planes along the longitudinal axis of the microstrip line. One side of the ground plane is etched to create a loop-like path for the current flow. This induces one sense of CP and the vertical/horizontal current on the feedline and the shortened ground plane contribute to the axial ratio bandwidth. To alter the sense of polarization, the position of the coplanar ground planes is switched with respect to the excitation line. To implement polarization and spatial diversity, the two antennas are placed in a parallel formation with the spatial distance of $0.29\lambda_0$. The antenna features a wide impedance bandwidth, AR bandwidth, stable bidirectional/unidirectional radiation pattern, low level of ECC and high diversity gain. The antenna covers a large frequency spectrum and it is suitable for applications requiring bidirectional/unidirectional radiation characteristics.

ACKNOWLEDGMENT

The authors would like to thank Dassault Systemes, France, for making CST Microwave Studio available.

REFERENCES

[1] D. Muirhead, M. A. Imran, and K. Arshad, "A survey of the challenges, opportunities and use of multiple antennas in current and future 5G small cell base stations," *IEEE Access*, vol. 4, pp. 2952–2964, 2016.
[2] F. A. Dicandia, S. Genovesi, and A. Monorchio, "Analysis of the performance enhancement of MIMO systems employing circular polarization," *IEEE Trans. Antennas Propag.*, vol. 65, no. 9, pp. 4824–4835, Sep. 2017.
[3] J. Malik, A. Patnaik, and M. V. Kartikeyan, "Novel printed MIMO antenna with pattern and polarization diversity," *IEEE Antennas Wireless Propag. Lett.*, vol. 14, pp. 739–742, 2015.
[4] S. M. Mikki and Y. M. M. Antar, "On cross correlation in antenna arrays with applications to spatial diversity and MIMO systems," *IEEE Trans. Antennas Propag.*, vol. 63, no. 4, pp. 1798–1810, Apr. 2015.
[5] A. Boukarkar, X. Q. Lin, Y. Jiang, L. Y. Nie, P. Mei, and Y. Q. Yu, "A miniaturized extremely close-spaced four-element dual-band MIMO antenna system with polarization and pattern diversity," *IEEE Antennas Wireless Propag. Lett.*, vol. 17, no. 1, pp. 134–137, Jan. 2018.
[6] M. S. Sharawi, M. Ikram, and A. Shamim, "A two concentric slot loop based connected array MIMO antenna system for 4G/5G terminals," *IEEE Trans. Antennas Propag.*, vol. 65, no. 12, pp. 6679–6686, Dec. 2017.
[7] P. Wang, H. Wang, L. Ping, and X. Lin, "On the capacity of MIMO cellular systems with base station cooperation," *IEEE Trans. Wireless Commun.*, vol. 10, no. 11, pp. 3720–3731, Nov. 2011.
[8] Z. Qin, M. Zhang, J. Wang, and W. Geyi, "Printed eight-element MIMO system for compact and thin 5G mobile handest," *Electron. Lett.*, vol. 52, no. 6, pp. 416–418, Mar. 2016.
[9] S. Shoaib, I. Shoaib, N. Shoaib, X. Chen, and C. G. Parini, "Design and performance study of a dual-element multiband printed monopole antenna array for MIMO terminals," *IEEE Antennas Wireless Propag. Lett.*, vol. 13, pp. 329–332, 2014.
[10] I. Nadeem and D.-Y. Choi, "Study on mutual coupling reduction technique for MIMO antennas," *IEEE Access*, vol. 7, pp. 563–586, 2019.
[11] J. Deng, J. Li, L. Zhao, and L. Guo, "A dual-band Inverted-F MIMO antenna with enhanced isolation for WLAN applications," *IEEE Antennas Wireless Propag. Lett.*, vol. 16, pp. 2270–2273, 2017.
[12] Y. Sharma, D. Sarkar, K. Saurav, and K. V. Srivastava, "Three-element MIMO antenna system with pattern and polarization diversity for WLAN applications," *IEEE Antennas Wireless Propag. Lett.*, vol. 16, pp. 1163–1166, 2017.
[13] C. B. Dietrich, K. Dietze, J. R. Nealy, and W. L. Stutzman, "Spatial, polarization, and pattern diversity for wireless handheld terminals," *IEEE Trans. Antennas Propag.*, vol. 49, no. 9, pp. 1271–1281, Sep. 2001.
[14] G. Wolosinski, V. Fusco, U. Naeem, and P. Rulikowski, "Pre-matched eigenmode antenna with polarization and pattern diversity," *IEEE Trans. Antennas Propag.*, vol. 67, no. 8, pp. 5145–5153, Aug. 2019.
[15] E. A. Soliman, W. De Raedt, and G. A. E. Vandenbosch, "Reconfigurable slot antenna for polarization diversity," *J. Biomaterials Sci., Polym. Ed.*, vol. 23, no. 7, pp. 905–916, May 2009.
[16] P. Kyritsi, D. C. Cox, R. A. Valenzuela, and P. W. Wolniansky, "Effect of antenna polarization on the capacity of a multiple element system in an indoor environment," *IEEE J. Sel. Areas Commun.*, vol. 20, no. 6, pp. 1227–1239, Aug. 2002.
[17] U. Ullah and S. Koziel, "Design and optimization of a novel miniaturized low-profile circularly polarized wide-slot antenna," *J. Electromagn. Waves Appl.*, vol. 32, no. 16, pp. 2099–2109, Nov. 2018.
[18] U. Ullah and S. Koziel, "A geometrically simple compact wideband circularly polarized antenna," *IEEE Antennas Wireless Propag. Lett.*, vol. 18, no. 6, pp. 1179–1183, Jun. 2019.
[19] U. Ullah, S. Koziel, and I. B. Mabrouk, "Rapid redesign and Bandwidth/Size tradeoffs for compact wideband circular polarization antennas using inverse surrogates and fast EM-based parameter tuning," *IEEE Trans. Antennas Propag.*, vol. 68, no. 1, pp. 81–89, Jan. 2020.
[20] K. O. Gyasi, G. Wen, D. Inserra, Y. Huang, J. Li, A. E. Ampoma, and H. Zhang, "A compact broadband cross-shaped circularly polarized planar monopole antenna with a ground plane extension," *IEEE Antennas Wireless Propag. Lett.*, vol. 17, no. 2, pp. 335–338, Feb. 2018.
[21] M. Ain, U. Ullah, and Z. Ahmad, "Bi-polarized dual-segment rectangular dielectric resonator antenna," *IETE J. Res.*, vol. 59, no. 6, p. 739, 2013.
[22] Rashmi, A. Kumar, K. Saraswat, and A. Kumar, "Wideband circularly polarized parasitic patches loaded coplanar waveguide-fed square slot antenna with grounded strips and slots for wireless communication systems," *AEU - Int. J. Electron. Commun.*, vol. 114, Feb. 2020, Art. no. 153011.
[23] P.-Y. Qin, Y. J. Guo, and C.-H. Liang, "Effect of antenna polarization diversity on MIMO system capacity," *IEEE Antennas Wireless Propag. Lett.*, vol. 9, pp. 1092–1095, 2010.
[24] R.-L. Li, V. F. Fusco, and H. Nakano, "Circularly polarized open-loop antenna," *IEEE Trans. Antennas Propag.*, vol. 51, no. 9, pp. 2475–2477, Sep. 2003.
[25] H. T. Chattha, "4-port 2-Element MIMO antenna for 5G portable applications," *IEEE Access*, vol. 7, pp. 96516–96520, 2019.
[26] U. Ullah, I. B. Mabrouk, and S. Koziel, "Enhanced-performance circularly polarized MIMO antenna with Polarization/Pattern diversity," *IEEE Access*, vol. 8, pp. 11887–11895, 2020.
[27] H. Li, S. Sun, B. Wang, and F. Wu, "Design of compact single-layer textile MIMO antenna for wearable applications," *IEEE Trans. Antennas Propag.*, vol. 66, no. 6, pp. 3136–3141, Jun. 2018.

UBAID ULLAH received the M.Sc. and Ph.D. degrees in electrical and electronic engineering from Universiti Sains Malaysia, in 2013 and 2017, respectively. From late 2017 to early 2019, he was with the Engineering Optimization and Modeling Center, School of Science and Engineering, Reykjavik University, Iceland. He is currently with Al Ain University, Abu Dhabi, United Arab Emirates. His research interests include antenna theory, small antennas, antenna polarization, dielectric resonators, waveguides, millimeter-wave antenna designs, multiple-input multiple-output (MIMO) antenna systems, EM-simulation-driven design, numerical analysis, and microwave circuit design and optimization. He was awarded the prestigious Global Fellowship and the Outstanding Student Award.

ISMAIL BEN MABROUK (Senior Member, IEEE) received the B.A.Sc. and M.A.Sc. degrees in electrical engineering from the University of Lille, Lille, France, in 2006 and 2007, respectively, and the Ph.D. degree in electrical engineering from the University of Quebec, Canada, in 2012. From 2007 to 2009, he was with Huawei Technologies, Paris, France. He joined the Wireless Devices and Systems (WiDeS) Group, University of Southern California, Los Angeles, CA, USA, in 2012. He is currently an Assistant Professor with the Al Ain University of Science and Technology, Abu Dhabi, UAE. His research activities have been centered on propagation studies for multiple-input and multiple-output (MIMO) systems, measurement campaigns in special environments, WBAN, and antenna design at the millimeter-wave and THz frequencies.

SLAWOMIR KOZIEL (Senior Member, IEEE) received the M.Sc. and Ph.D. degrees in electronic engineering from the Gdansk University of Technology, Poland, in 1995 and 2000, respectively, and the M.Sc. degree in theoretical physics and the M.Sc. and Ph.D. degrees in mathematics from the University of Gdansk, Poland, in 2000, 2002, and 2003, respectively. He is currently a Professor with the School of Science and Engineering, Reykjavík University, Iceland. His research interests include CAD and modeling of microwave and antenna structures, simulation-driven design, surrogate-based optimization, space mapping, circuit theory, analog signal processing, evolutionary computation, and numerical analysis.

MUATH AL-HASAN (Senior Member, IEEE) received the B.A.Sc. degree in electrical engineering from the Jordan University of Science and Technology, Jordan, in 2005, the M.A.Sc. degree in wireless communications from Yarmouk University, Jordan, in 2008, and the Ph.D. degree in telecommunication engineering from the Institut National de la Recherche Scientifique (INRS), Université du Québec, Canada, 2015. From 2013 to 2014, he was with Planets Inc., CA, USA. He joined Concordia University, Canada, as a Postdoctoral Fellowship, in May 2015. He is currently an Assistant Professor with Al Ain University, United Arab Emirates. His current research interests include antenna design at millimeter-wave and Terahertz frequencies, electromagnetic bandgap (EBG) structures, and channel measurements in multiple-input and multiple-output (MIMO) systems.